

NUMERICAL MODELING OF TEMPERATURE FIELD ACROSS A PRISMATIC ELEMENT OF A SOIL

Agberegha, Orobome Larry^{1#}, Nwigbo, Chuka Solomon^{2*}, Enibe, Samuel Ogbonna^{3?}, Agha, Stephen^{4\$} and Anyanwu, S. Ikechukwu⁺⁵

^{1#}Department of Mechanical Engineering, Federal University of Petroleum Resources Effurun, Nigeria - 330102;

^{2*}Department of Mechanical Engineering, Nnamdi Azikiwe University; Awka, Nigeria - 420110

^{3?}Department of Mechanical Engineering, University of Nigeria, Nsukka; Nigeria - 410001

^{4\$}Department of Mechanical Engineering, School of Engineering and Materials Science, Queen Mary University of London, United Kingdom - 56273

⁺⁵ State Key Laboratory of Engines, Tianjin University, 92 Wejin Rd., Tianjin 300072, China – 300072

Corresponding Author Email: Orobome_agberegha@yahoo.com

ABSTRACT

Temperature distribution in the soil around the study area [Coordinates 5⁰31'N 5045'E/5.517⁰N 5.750⁰E] are simulated by a two-dimensional model based on conduction heat transfer, with the help of SCILAB, Microsoft Excel and minitab16 user interface tool. In this system, heat is transferred, basically from the surface of the earth dominantly by conduction, convection, or both. However, the modeled developed, had convective heat transfer neglected. "The spatial variation of the magnitude of conductive heat transfer represented by lateral variation of observed surface heat flow values is heavily related to the subsurface temperature distribution, the pattern of which is directly controlled by the variation of rock thermal conductivity values." Therefore, it may be inferred that the information about subsurface temperature distribution may provide insight for the interpretation of the thermal structure of a computational space. This insight, it is believed, could help in studies of the negative impact bush burning has on the mineral and soil structure. In this research, numerical forward modeling procedure of 2-D conductive heat transfer using finite difference solution of the steady state heat conduction equation via a Gauss-Seidel scheme was performed. The main physical parameters used as the input in the modeling procedure are rock thermal conductivity values as well as temperature boundary conditions. The modeling scheme was applied on an elemental portion of the substrate, soil, by using appropriate thermal conductivities and temperature boundary conditions for the abstracted computational space. The results, from the numerical studies and the modeling procedure, adopted, were able to effectively characterize the thermal structure and surface heat flow patterns of the computational space, soil substrate. Results from the numerical simulation shows that temperatures on the soil substrate represented by a rectangular plate, at steady state with known boundary temperatures using three different techniques gave the same temperatures, validating the results.

1.0 INTRODUCTION

The soil is the giver and sustainer of life, directly for plants and indirectly, for man and every other living thing. Ezio Ranieri et al. 2016 defined soil as a point of concentration and recovery of toxic compounds, chemicals, salts, radioactive materials, or disease causing agents, which have adverse effects on plant growth and animal health.

Bush burning, which directly affects the soil, comes with its attendant temperature increase, which in turn affects the life of plants and its minerals (Chandler and others 1983). While

some researchers have averred that bush burning, indeed, aids the sprouting of new species of plants Seaver and Clark (1912); Garcia-Corona et al 2004; Giovannini et al (1990) have had profound research into the effects of temperature/heat flux arising from the practice of bush burning. Bush burning comes with its attendant temperature increase, which in turn affects the life of plants and its minerals. Interestingly, Fire acts as a rapid mineralizing agent (St. John and Rundel 1976) that releases nutrients instantaneously as contrasted to natural decomposition processes, which may require years or, in some cases, decades. DeBano, (1991). Heating or burning has a wide variety of effects on soils, the magnitude of which is determined largely by the temperature to which the soil is heated and on soil properties. Kitur and Frye, 1983. Bush burning is an ancient process; different geographies have various philosophies for carrying out that act. This work seeks to estimate the temperature field in open exposed to bush burning.

Combustion of biomass and soil organic matter also results in the release of gases and other pollutants into the atmosphere Zavala et al. 2014. Combustion, or bush burning is a complex interplay of fire(fuel, heat and material), soil(the substrate), hydrology and nutrient recycling.

The following is affected – positively or negatively –by bush burning: Organic matter, Nitrogen and Sulphur; phosphorus and cation (NH_4^+ , K^+ , Ca^{++}); soil microorganism DeBano, (1991).

2.0 Study Area

The study area is located in Uvwie Local Government Area of Delta State. Coordinates $5^{\circ}31'N$ $5045'E/5.517^{\circ}N$ $5.750^{\circ}E$. The region experiences moderate rainfall and moderate humidity for most part of the year. The climate is equatorial and is marked by two distinct seasons: the dry season and the rainy season. The dry season lasts from about November to April and is significantly marked by the cool "harmattan" dusty haze from the north-east winds. The rainy season spans May to October with a brief dry spell in August, but it frequently rains even in the dry season. The area is characterized by tropical equatorial climate with mean annual temperature of 32.8°C and annual rainfall amount of 2673.8 mm. There are high temperatures of 36°C and 37°C . The natural vegetation is of rainforest with swamp forest in some areas. The forest is rich in timber trees, palm trees, as well as fruit trees.



Figure 1.0: Swampy Mangrove Vegetation showing crude oil carrying pipeline

3.0 Methodology

The boundary conditions for the computational space – the soil substrate was determined by a pyrometer, which measured the temperature of radiative heat transfer from the fire; and [Large Dial Thermometer](#), which recorded the temperature of the substrate. Temperature distribution in the soil around the study area [Coordinates $5^{\circ}31'N$ $5045'E/5.517^{\circ}N$ $5.750^{\circ}E$] are simulated by a two-dimensional model based on conduction heat transfer, with the help of SCILAB, Microsoft Excel and minitab16 user interface tool. A 3-D numerical model to estimate the

internal temperature field was developed; this is converted to a 2-D model. Numerical forward modeling procedure of 2-D conductive heat transfer using finite difference solution of the steady state heat conduction equation via a Gauss-Seidel scheme was performed. The main physical parameters used as the input in the modeling procedure are rock thermal conductivity values as well as temperature boundary conditions. The modeling scheme was applied on an elemental portion of the substrate, soil, by using appropriate thermal conductivities and temperature boundary conditions for the abstracted computational space. The results, from the numerical studies and the modeling procedure, adopted, were able to effectively characterize the thermal structure and surface heat flow patterns of the computational space, soil substrate.

3.1 Numerical modeling of heat distribution in a 5 X 5 nodal problem

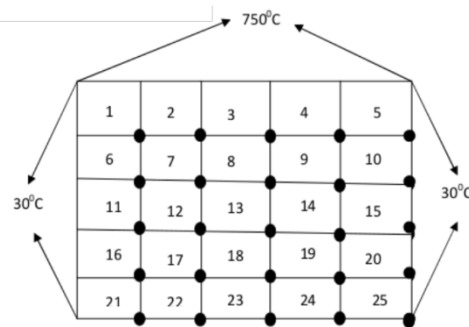


Figure 2: nomenclature for the prismatic element of the soil under numerical modeling
The governing partial differential equation in 3-D for the temperature field $T(x,y,z,t)$ is

$$\frac{\partial}{\partial x} \left[\lambda_x \frac{\partial T}{\partial x} \right] + \frac{\partial}{\partial y} \left[\lambda_y \frac{\partial T}{\partial y} \right] + \frac{\partial}{\partial z} \left[\lambda_z \frac{\partial T}{\partial z} \right] + I(x, y, z, t) = c \frac{\partial T}{\partial t} \quad [1]$$

In cylindrical coordinates, the heat flow or temperature field may be modeled using rationally symmetrical heat flow

$$\frac{1}{r} \frac{\partial}{\partial r} \left(\lambda \cdot r \frac{\partial T}{\partial r} \right) + \frac{\partial}{\partial z} \left(\lambda \frac{\partial T}{\partial z} \right) = c \frac{\partial T}{\partial t} \quad [2]$$

For the 2-D heat flow, the governing equation can be modeled ignoring heat flow along the z-axis; equation 1 reduces to:

$$\frac{\partial}{\partial x} \left[\lambda_x \frac{\partial T}{\partial x} \right] + \frac{\partial}{\partial y} \left[\lambda_y \frac{\partial T}{\partial y} \right] + I(x, y, t) = c \frac{\partial T}{\partial t} \quad [3]$$

Where I [W/m³] is the rate of internal heat generation. The thermal conductivity in the x, y – directions are denoted by λ_x and λ_y , respectively. The volumetric heat capacity is denoted by c [J/(m³k)], which is the density times the specific heat capacity ($c = \rho \cdot c_p$). The thermal conductivity in the two dimensions (or coordinates) are usually the same $\lambda_x = \lambda_y$. The internal heat generation is negligible in most literatures. However, in this work it is taken as the source of heat since in steady state heat conduction, the term $\frac{\partial T}{\partial t}$ is zero or that heat transfer is independent of time.

From the afore-analysis, equation 1 could be written thus

$$\lambda_x \frac{\partial^2 T}{\partial x^2} + \lambda_y \frac{\partial^2 T}{\partial y^2} + \lambda_z \frac{\partial^2 T}{\partial z^2} + I(x, y, z, t) = c \frac{\partial T}{\partial t} \quad [4]$$

If we assume that $\lambda_x = \lambda_y = \lambda_z$, we may write

$$\frac{\partial^2 T}{\partial x^2} + \frac{\partial^2 T}{\partial y^2} + \frac{\partial^2 T}{\partial z^2} + \frac{1}{\lambda} I(x, y, z, t) = \frac{c}{\lambda} \frac{\partial T}{\partial t} \quad [5]$$

If we further assume that no heat generation occurs in the computational space, we have that

$$\frac{\partial^2 T}{\partial x^2} + \frac{\partial^2 T}{\partial y^2} + \frac{\partial^2 T}{\partial z^2} = \frac{c}{\lambda} \frac{\partial T}{\partial t} \quad [6]$$

If we also consider the heat flow as one of steady-state conduction, we have

$$\frac{\partial^2 T}{\partial x^2} + \frac{\partial^2 T}{\partial y^2} + \frac{\partial^2 T}{\partial z^2} = 0 \quad [7]$$

The forward finite difference formulation of the differential coefficients for the temperature differential wrt time is

$$\left(\frac{\partial T}{\partial t}\right)_{m+\frac{1}{2},n,o} \approx \frac{T_{m,n,o}^{p+1} - T_{m,n,o}^p}{\Delta t} \quad [8]$$

The finite difference formulation of the differential coefficients for the temperature differential wrt space coordinates x- axis is given as

$$\frac{\partial^2 T}{\partial x^2} \approx \frac{1}{(\Delta x)^2} [T_{m+1,n,o}^p + T_{m-1,n,o}^{p+1} - 2T_{m,n,o}^p] \quad [9]$$

The finite difference formulation of the differential coefficients for the temperature differential wrt space coordinates y- axis is given as

$$\frac{\partial^2 T}{\partial y^2} \approx \frac{1}{(\Delta y)^2} [T_{m,n+1,o}^p + T_{m,n-1,o}^{p+1} - 2T_{m,n,o}^p] \quad [10]$$

The finite difference formulation of the differential coefficients for the temperature differential wrt space coordinates z- axis is given as

$$\frac{\partial^2 T}{\partial z^2} \approx \frac{1}{(\Delta z)^2} [T_{m,n,o+1}^p + T_{m,n,o-1}^{p+1} - 2T_{m,n,o}^p] \quad [11]$$

It is to be noted that the superscripts designate the time increment. Substituting equations 8, 9, 10 and 11 into equations 6, we have

$$\begin{aligned} & \frac{[T_{m+1,n,o}^p + T_{m-1,n,o}^{p+1} - 2T_{m,n,o}^p]}{(\Delta x)^2} + \frac{[T_{m,n+1,o}^p + T_{m,n-1,o}^{p+1} - 2T_{m,n,o}^p]}{(\Delta y)^2} \\ & + \frac{[T_{m,n,o+1}^p + T_{m,n,o-1}^{p+1} - 2T_{m,n,o}^p]}{(\Delta z)^2} \\ & = \frac{c}{\lambda} \left[\frac{T_{m,n,o}^{p+1} - T_{m,n,o}^p}{\Delta t} \right] \end{aligned} \quad [12]$$

For to simplify complex physics to simple physics one, we could assume that the increments along the x, y and z axis are equal: $\Delta x = \Delta y = \Delta z$, we simplify and get

$$\frac{\lambda \Delta x}{c(\Delta x)^2} [T_{m+1,n,o}^p + T_{m-1,n,o}^{p+1} + T_{m,n+1,o}^p + T_{m,n-1,o}^{p+1} + T_{m,n,o+1}^p + T_{m,n,o-1}^{p+1}] + \left[1 - \frac{6\lambda \Delta x}{c(\Delta x)^2}\right] T_{m,n,o}^p = T_{m,n,o}^{p+1} \quad [13]$$

We may, for the purpose of simplifying the problem, chose the time and space increment thus:

$$\frac{(\Delta x)^2}{6\lambda \Delta x} = 0 \quad [14]$$

We thus have

$$T_{m,n,o}^{p+1} = \frac{1}{6} [T_{m+1,n,o}^p + T_{m-1,n,o}^{p+1} + T_{m,n+1,o}^p + T_{m,n-1,o}^{p+1} + T_{m,n,o+1}^p + T_{m,n,o-1}^{p+1}] \quad [15]$$

It is observed from equation [15] that the temperature of the node (m,n,o) after time increment $p + 1$ is simply the mean of the six adjoining nodal temperatures at the beginning

of the time increment. It is to be noted that equation [15] is for interior nodal equation for the prismatic elemental substrates of the soil.

For the sole aim of simplification, this 3-D model could be transformed to a 2-D and further to a 1-D model by applying Bursa-Wolf model (King et al., 1985)

$$\begin{bmatrix} X_2 \\ Y_2 \\ Z_2 \end{bmatrix} = (1 + k) \begin{bmatrix} 1 & \varepsilon_z & -\varepsilon_y \\ -\varepsilon_z & 1 & \varepsilon_x \\ \varepsilon_y & -\varepsilon_x & 1 \end{bmatrix} \begin{bmatrix} X_1 \\ Y_1 \\ Z_1 \end{bmatrix} + \begin{bmatrix} f_x \\ f_y \\ f_z \end{bmatrix} \quad [16]$$

Or

$$X = (1 + k) * R * \ddot{X}_1 + \vec{t}_x \quad [17]$$

The transformation includes three translation components, t_x, t_y, t_z , three small rotations $\varepsilon_x, \varepsilon_y, \varepsilon_z$ and a scalar component k, which is derivation of the scale from unity (1+k) and is small enough to be expressed in ppm

Equation [15] collapses into 2-D, thus

$$\frac{[T_{m+1,n}^p + T_{m-1,n}^{p+1} - 2T_{m,n}^p]}{(\Delta x)^2} + \frac{[T_{m,n+1}^p + T_{m,n-1}^{p+1} - 2T_{m,n}^p]}{(\Delta y)^2} = \frac{c}{\lambda} \left[\frac{T_{m,n}^{p+1} - T_{m,n}^p}{\Delta t} \right] \quad 18$$

And further to this

$$\frac{[T_{m+1,n}^p + T_{m-1,n}^p - 2T_{m,n}^{p+1}]}{(\Delta x)^2} + \frac{[T_{m,n+1}^p + T_{m,n-1}^p - 2T_{m,n}^{p+1}]}{(\Delta y)^2} = 0 \quad [19]$$

Like in the case with 3-D modeling, we could assume equal increment on both side x and y – axis and further simplyfying, thus

$$T_{m+1,n}^p + T_{m,n-1}^{p+1} - 2T_{m,n}^p + T_{m,n+1}^p + T_{m,n-1}^{p+1} - 4T_{m,n}^{p+1} = 0 \quad [20]$$

$$T_{m,n}^{p+1} = \frac{1}{4} [T_{m+1,n}^p + T_{m,n-1}^{p+1} - 2T_{m,n}^p + T_{m,n+1}^p + T_{m,n-1}^{p+1}] \quad [21]$$

For a steady state, equation [21] reduces to equations [22]

3.2 Boundary conditions formulations

For the problem under consideration, the boundary conditions are:

$$\begin{aligned} \text{at } x = L, & \quad T = 30^{\circ}C \\ \text{at } x = 0, & \quad T = 0 \\ \text{at } y = 0, & \quad T = 0 \\ \text{at } y = H, & \quad T = 750^{\circ}C \end{aligned}$$

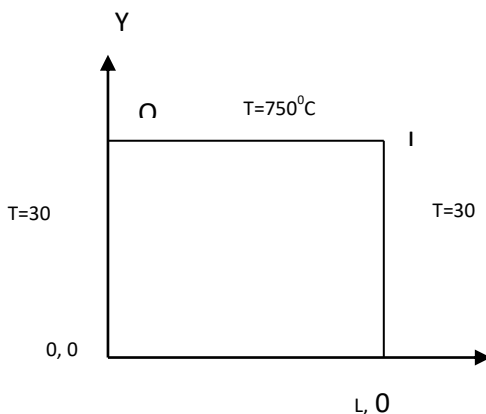


Figure 3: the elemental portion of the soil with temperature specified boundary conditions.

Hence only the temperatures at the interior surfaces need to be determined using equations [22]. These are the nodes numbered 7 –9, 12 – 14, and 17 – 19. For convenience, these nodes are renumbered 1 to 9 as shown in the table below.

Table 1.0: numerical node nomenclature

<i>Index old</i>	7	8	9	12	13	14	17	18	19
<i>Index new</i>	1	2	3	4	5	6	7	8	9

The general nodal equation, after applying equation [21], the temperatures at the selected nodes are determined by inspection using the expressions below:

$$\left. \begin{aligned}
 Tr(1) &= \frac{1}{4} [750 + Tr(4) + 30 + Tr(2)] \\
 Tr(2) &= \frac{1}{4} [750 + Tr(5) + Tr(1) + Tr(3)] \\
 Tr(3) &= \frac{1}{4} [750 + Tr(6) + Tr(2) + 30] \\
 Tr(4) &= \frac{1}{4} [Tr(1) + Tr(7) + 30 + Tr(5)] \\
 Tr(5) &= \frac{1}{4} [Tr(2) + Tr(8) + Tr(4) + Tr(6)] \\
 Tr(6) &= \frac{1}{4} [Tr(3) + Tr(9) + Tr(5) + 30] \\
 Tr(7) &= \frac{1}{4} [Tr(4) + 30 + 30 + Tr(8)] \\
 Tr(8) &= \frac{1}{4} [Tr(5) + 30 + Tr(7) + Tr(9)] \\
 Tr(9) &= \frac{1}{4} [Tr(6) + 30 + Tr(8) + 30]
 \end{aligned} \right\} \quad [22]$$

The nine equations (equation [22]) for these temperatures could be solved iteratively using the Gauss-Seidel algorithm as shown appendix 1. First, the equations for the nodal temperatures are expressed using the function myfunction. Then the function gaussSeidel (shown in listing A.1) is called to perform the calculations without the use of relaxation technique. The result is obtained after 39 iterations. Next, to reduce the number of iterations, the concept of relaxation is introduced. First, the equation is reformulated as a matrix equation of the form Ax = b, where

$$A = \begin{bmatrix}
 -4 & 1 & 0 & 1 & 0 & 0 & 0 & 0 & 0 \\
 1 & -4 & 1 & 0 & 1 & 0 & 0 & 0 & 0 \\
 0 & 1 & -4 & 0 & 0 & 1 & 0 & 0 & 0 \\
 1 & 0 & 0 & -4 & 1 & 0 & 1 & 0 & 0 \\
 0 & 1 & 0 & 1 & -4 & 1 & 0 & 1 & 0 \\
 0 & 0 & 1 & 0 & 1 & -4 & 0 & 0 & 1 \\
 0 & 0 & 0 & 1 & 0 & 0 & -4 & 1 & 0 \\
 0 & 0 & 0 & 0 & 1 & 0 & 1 & -4 & 1 \\
 0 & 0 & 0 & 0 & 0 & 1 & 0 & 1 & -4
 \end{bmatrix}
 \quad
 B = \begin{bmatrix}
 -750 \\
 -750 \\
 -750 \\
 -30 \\
 0 \\
 -30 \\
 -60 \\
 -30 \\
 -60
 \end{bmatrix}$$

The arrays A and b are coded in the function myfunction2. The relaxation technique is also indicated in the function (the functionrelaxation is shown in listing A.2). The gaussSeidel algorithm is then employed to solve the equation, and the results obtained are the same as before but with only 19 iterations. The final value of the relaxation parameter is ! =

1:0552733. Finally, the problem is also solved using the left division operator $x = A \setminus b$. The results using the three methods are shown in table 1.1, and they are seen to be the same. The distribution of the temperatures on the plate is shown in table 1.2.

4.0 RESULTS AND DISCUSSION

Temperatures on the soil substrate represented by a rectangular plate, at steady state with known boundary temperatures using three different techniques (figures 3, 4, 6 and 7).

Temperature distribution on soil substrate

At the base of the soil substrate, the temperature increased from 81.42857°C to 100.7143°C ; Deherain and Demousse (1896) asserts that for a temperature increase of this range, thermophilic organisms activities increases, which in turn decreases respiration and this temperature has effect on the soil. Both investigations were restricted to CO_2 evolution, which need not be fully indicative of the metabolism of the soil population. Kitur and Frye. 1983 observes that at a temperature of slightly above 100.7143°C , the soil's pH decreases; conversely, at the temperature between 200 or 250°C pH increases. Organic matter and extractable Mg decreased while extractable NH_4^+ and Mn and electrical conductivity (EC) increased greatly with heating. The effects on soil-test P and K and extractable Ca were small and variable, but the soils were already high in these elements. Increases in extractable N and Mn, EC, and pH probably came from both the destruction of soil organic matter and release from inorganic compounds in the soils. Heating soils to 110°C resulted in greater growth of both corn and millet, but heat treatments of 200 and 250°C suppressed growth. The increase in the growth of corn and millet was attributed primarily to moderate increases in extractable NH_4^+ at 110°C . The suppression of growth with heat treatments of 200 and 250°C was thought to be due largely to excessive amounts of NH_4^+ . Extensive work on NH_4^+ shows that certain levels of this form of N may be toxic to plants. Heating of soil was shown to be both beneficial and detrimental to the growth of plants. Crops may benefit from nutrients released when soils are heated, provided the amounts are not excessive.

Also, Garcia-Corona et al. 2004 observes that heating at below 220°C was found to have no adverse effect on aggregation-related soil properties; rather, water aggregate stability increased over the temperature range $170\text{--}220^{\circ}\text{C}$. On the other hand, water repellency increased over that range and resulted in substantially decreased hydraulic conductivities up to 220°C . At soil temperature of between $380\text{--}460^{\circ}\text{C}$, the combustion of organic matter favoured dry disaggregation and reduced water aggregate stability. Although water repellency disappeared at such temperatures, the hydraulic conductivity remained very low. The reduced hydraulic conductivity is the principal adverse effect of soil heating by fires, as the decreased infiltration capacity facilitates surface runoff and facilitates soil erosion.

Giovannini et al (1990) observes that the heating of soil had a variable effect on pH, with a decrease up to 220°C and a sharp increase after 700°C ; It was also observed that heating produced a continuous decrease of the cation exchange capacity in both soils. The effect of the heat on organic matter content, total nitrogen, and organic phosphorus was similar, with a little decrease up to 220°C ; beyond this value, it was reported from the results, that the organic matter was burned up, the total nitrogen was volatilized, and the organic phosphorus was mineralized and transformed into the inorganic form. However, the $\text{N} - \text{NH}_4$ increased up to 220°C and then decreased very sharply; at 460°C it was barely detectable. It would seem, in comparison with Giovannini et al (1990), water- extractable cations would show

various behaviours. From row 3, columns 2, 3 and 4, the temperature at these nodal points we could infer that the heating had no effect on plant and root growth and dry matter production.

For temperatures approaching 100°C, the free moisture is vaporized as soon as the temperature approaches 100°C. Lignin and hemicellulose begin to degrade at temperatures between 130 and 190°C. Reactions occurring at temperatures below 200°C are endothermic (reactions that require the absorption of heat). Decomposition of lignin and hemicellulose becomes rapid at 200°C with cellulose undergoing chemical dehydration at 280°C. About 35 percent of the total weight loss occurs before soil OM reaches 280°C. Once soil temperatures exceed 280°C, exothermic reactions (those reactions that produce heat) predominate and OM is ignited. When the surface temperature of soil OM reaches 500 to 600°C, glowing combustion occurs if oxygen is not excluded from the char surface. Flaming then occurs and boosts temperatures from 800 to 1,500°C. Above 1,000°C carbon (C) is consumed at the surface as rapidly as char is produced. DaBano (1991).

Table 1.1: Temperatures on a rectangular plate at steady state with known boundary temperatures for example [1.1] using three different techniques

GaussSeidel 1	GaussSeidel 2	Backclass operator
338.57143	338.57143	338.57143
409.28571	409.28571	409.28571
338.57143	338.57143	338.57143
165	165	165
210	210	210
165	165	165
81.428571	81.428571	81.428571
100.71429	100.71429	100.71429
81.428571	81.428571	81.428571

Table 1.2: Temperature distribution on a rectangular plate at steady state with known boundary temperatures for example [1.1]

750	750	750	750	750
30	338.57143	409.28571	338.57143	30
30	165	210	165	30
30	81.428571	100.71429	81.428571	30
30	30	30	30	30

Figure 3: temperature on a rectangular plate at steady state with known boundary temperatures using three different techniques.

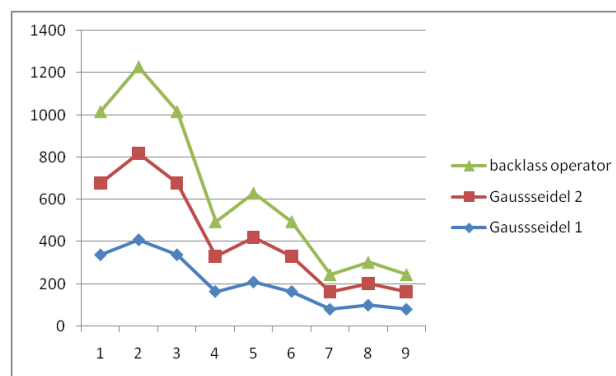


Figure 4: plot of temperature on the substrate using three different techniques.

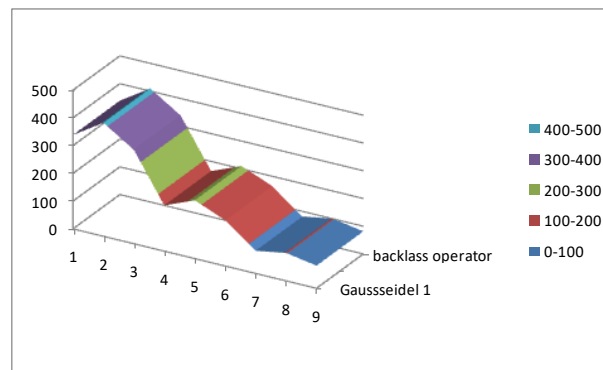


Figure 5: 3D plot temperature of the soil substrate

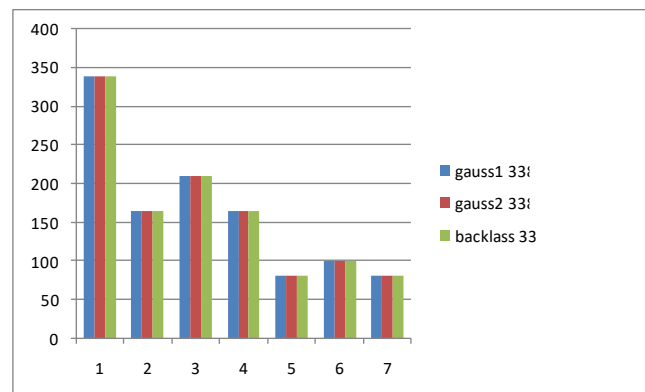


Figure 6: bar chart representing the

REFERENCE

1. Kitur, B.K., and W.W. Frye. (1983). Effects of heating on soil chemical properties and growth and nutrient composition of corn and millet. *Soil, Sci. Soc. Am. J.* 47:91-94.
2. DEHERAINP.,P and DEMOUSSE (1896), Sur l'oxydation de la matikre organique du sol. *Ann. Agron.* 22, 30537.
3. R. Garcia-Corona,E. Benito, E. de Blas and M. E. Varela (2004), Effects of Heating on some Soil Physical properties related to its Hydrological Behaviour in two North-Western Spanish Soils, *International journal of Wildland Fire*, 13, 195-199
4. G. Giovanni, S. Lucchesi and M. Giaxhetti (1990), Effects of Heating on Some Chemical Parameters Related to Soil Fertility and Plant Growth, C. N. R., Institute for Soil Chemistry, Italy.
5. Chandler, Craig; Cheney, Phillip; Thomas, Philip; Trabaud, Louis; Williams, Dave. (1983). *Fire in forestry. Vol. 1: forest fire behavior and effects.* New York: John Wiley & Sons. 450 p.
6. DeBano, Leonard F. (1991). The effect of fire on soil properties. In: Harvey, Alan E.; Neuenschwander, Leon F., compilers. *Proceedings-management and productivity of western-montane forest soils; 1990 April 10-12; Boise, ID. Gen. Tech. Rep. INT-280.* Ogden, UT: U.S. Department of Agriculture, Forest Service, Intermountain Research Station. p. 151-156.
7. J. P. Holman (2010), *Heat Transfer, Tenth Edition.*

5. 0 Appendix

Listing 1.1: SCILAB code to determine the temperature distribution on a rectangular plate at steady state with known boundary temperatures

```

myfile = "5 node .s ce" ; // file name
2 T(1, 1:25) = 30; // initialise temperatures at 30 degrees C
T(1, 1:5) = 750; // temperatures at the top face
4 index = [7 8 9 12 13 14 17 18 19; // index for full grid
1 2 3 4 5 6 7 8 9]; // indices for
the selected grids
6 Tr(index(2, :)) = [T(index(1, :))]'; // initialise temperatures for
the selected grids as a column vector
// solution with Gauss Seidel
8
function [Tr] = myfunction(Tr, omega)
10 Tr(1) = (750 + Tr(4) + 30 + Tr(2)) / 4; // temperature at node 1
Tr(2) = (750 + Tr(5) + Tr(1) + Tr(3)) / 4; // temperature at node 2
12 Tr(3) = (750 + Tr(6) + Tr(2) + 30) / 4; // temperature at node 3
Tr(4) = (Tr(1) + Tr(7) + 30 + Tr(5)) / 4; // temperature at node 4
14 Tr(5) = (Tr(2) + Tr(8) + Tr(4) + Tr(6)) / 4; // temperature at node 5
Tr(6) = (Tr(3) + Tr(9) + Tr(5) + 30) / 4; // temperature at node 6
16 Tr(7) = (Tr(4) + 30 + 30 + Tr(8)) / 4; // temperature at node 7
Tr(8) = (Tr(5) + 30 + Tr(7) + Tr(9)) / 4; // temperature at node 8
18 Tr(9) = (Tr(6) + 30 + Tr(8) + 30) / 4; // temperature at node 9
end function
20 omega1 = 1; // a relaxation parameter. Setting this as 1 implies
[Tr1, numIter, omega1] = gaussSeidel("myfunction", Tr); // solve
the equation with gauss Seidel iteration
22 function [Tr, A, b] = myfunction2(Tr, omega) // alternative
formulation in matrix form
A = [4 1 0 1 0 0 0 0 0; // row 1
24 1 4 1 0 1 0 0 0 0; // row 2
0 1 4 0 0 1 0 0 0; // row 3
26 1 0 0 4 1 0 1 0 0; // row 4
0 1 0 1 4 1 0 1 0; // row 5
28 0 0 1 0 1 4 0 0 1; // row 6
0 0 0 1 0 0 4 1 0; // row 7
30 0 0 0 0 1 0 1 4 1; // row 8
0 0 0 0 0 1 0 1 4 // row 9
32 ]
b = [780 750 780 30 0 30 60 30 60]'; // vector b
34 Tr = relaxation(A, b, Tr, omega1); // recompute the solution
matrix with the value of the relaxation
end function
36 omega2 = 1; // initialise
[Tr2, A, b] = myfunction2(Tr, omega2); // extract the
38 Tr2 = A \ b; // solve with the backslash operator
// disp("Pause at line 41 of programme 5 node .s ce"); pause
40 [Tr3, numIter3, omega3] = gaussSeidel("myfunction2", Tr); // solve
e

```

```

the equation with Gauss Seidel iteration
42 T(index(1,:))=Tr1;//assign to the full temperature matrix
result=[matrix(T,5,5)]';//arrange the results in a 5 by 5
matrix and transpose
44 disp(result,"result=");//display the result
mydir=get_absolute_file_path(myfile);//get full file path
46 filename1=mydir+basename(myfile)+"result.csv";//
csvWrite(result,filename1);//save result as a csv file
48 filename=basename(myfile)+"□result.tex";//output filename
data=string2latex(mydir,filename,string(result));//save
file in LaTeX format
50 result2=[numIter omega1 ;
numIter3 omega3]';//output of number of
iterations and omega
52 header=["Number of iterations " "omega "];//
outdata2=[header;string(result2)];//add as second column
54 filename2=basename(myfile)+"□result2.tex";//output filename
data2=string2latex(mydir,filename2,outdata2);//save file in
LaTeX format
56
result3=[Tr1 Tr3 Tr2]';//results from the 3 methods
58 header3=["Gauss Seidel1 " "Gauss Seidel2 " "Backslash operator
"];//
outdata3=[header3;[string(result3)]];//add as second column
60 filename3=basename(myfile)+"□result3.tex";//output filename
data3=string2latex(mydir,filename3,outdata3);//save file in
LaTeX format

```